Superconductivity of H_3S doped with light elements

Hongyi Guan [1], Ying Sun [1] and Hanyu Liu [1,2,3,*]

[1] *International Center for Computational Method & Software and State Key Laboratory of Superhard Materials, College of Physics, Jilin University, Changchun 130012, China*

[2] *Key Laboratory of Physics and Technology for Advanced Batteries (Ministry of Education), College of Physics, Jilin University, Changchun 130012, China*

[3] *International Center of Future Science, Jilin University, Changchun 130012, China*

(Received 20 August 2021; accepted 12 October 2021; published 10 November 2021)

Pressurized hydrogen-rich compounds, which could be viewed as precompressed metallic hydrogen, exhibit high superconductivity, thereby providing a viable route toward the discovery of high-temperature superconductors. Of particular interest is to search for high-temperature superconductors with low stable pressure in terms of pressure-stabilized hydrides. In this work, with the aim of obtaining high-temperature superconducting compounds at low pressure, we attempt to study the doping effects for high-temperature superconductive H_3S with supercells up to 64 atoms using first principle electronic structure simulations. As a result of various doping, we found that Na doping for H_3S could lower the dynamically stable pressure by 40 GPa. The results also indicate that P doping could enhance the superconductivity of the H_3S system, which is in agreement with previous calculations. Moreover, our work proposed an approach that could reasonably estimate the superconducting critical temperature (T_c) of a compound containing a large number of atoms, saving the computational cost significantly for large-scale elements-doping superconductivity simulations.

DOI: 10.1103/PhysRevResearch.3.043102

I. INTRODUCTION

The search for the high-temperature superconducting hydrides at high pressures has attracted attention in the condensed matter physics field. In this regard, many hydrides with relatively high T_c were identified under high pressure [1–15]. Among these high-temperature superconducting hydrides, the theoretically predicted H_3S with T_c of 203 K [1–3] and LaH_{10} with T_c of 250–260 K in [5–8], as well as CaH_6 being the first example of clathrate hydrides ever predicted [16–18], were experimentally synthesized. Recently, the carbonaceous sulfur hydride was found to possess extremely high superconductivity with a T_c as high as 288 K at 267 GPa [12], however, the actual crystal structure and the mechanisms of such extremely high superconductivity remains unclear and missing [19–23].

Structure searches below 200 GPa were performed for the C-S-H system [19–21,24,25], while no high superconductive structure is yet identified. Later, it was reported that the high superconductivity in the C-S-H compound could be explained by the doping of C into the $Im\bar{3}m$ H_3S [21,26], whereas these simulations are based on the virtual crystal approximation (VCA) [27]. This approximation is employed with linearly mixed pseudopotentials and could not take the details of symmetry breaking and local distortions into account. These issues, in principle, could be addressed by performing the electronic simulations of doping carbon into a sufficiently large supercell of H_3S, if the computational power is allowed.

In this paper, we investigated the structures and physical properties of partially substituting sulfur by the light elements in $Im\bar{3}m$ H_3S with supercell approach at the pressure range 150–250 GPa by first-principle calculations. Our calculations mainly focus on $H_{24}S_7X$ and $H_{48}S_{15}X$, where X denotes the doping elements from H to Cl without He and Ne in the periodic table. As a result, we found that the Na doping could lower the dynamically stable pressure of 40 GPa compared to the parent H_3S system. Furthermore, the P doping could enhance the superconductivity of the parent H_3S system, which is ascribed to octahedra units $[SH_6]$ and $[PH_6]$. In addition, we proposed an estimation approach to investigate the low proportion C-doping effects at 260 GPa. The results suggest the estimated T_c is much lower than the room temperature.

II. COMPUTATIONAL DETAILS

The structural optimization was done by the Vienna Ab initio Simulation Package (VASP) [28], with pseudopotentials employing generalized gradient approximation (GGA) based Perdew-Burke-Ernzerhof (PBE) type exchange correlation functional [29] and the projector-augmented wave method [30]. Monkhorst $\boldsymbol{k}$ meshes [31] spacing $2\pi \times 0.1$ Å^{-1} was used to sample the first Brillouin zones. The electronic density of states was also computed by VASP with $20 \times 20 \times 20\,\boldsymbol{k}$ mesh and was analyzed by VASPKIT [32]. The phonon properties and superconducting properties were computed by

*hanyuliu@jlu.edu.cn

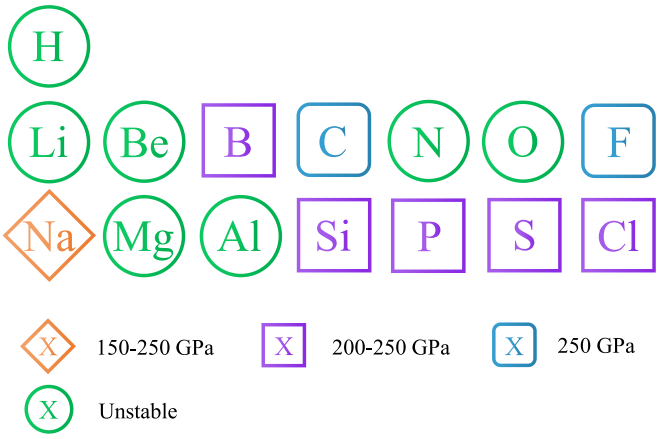

FIG. 1. Summary of dynamical stability and dynamically stable pressure ranges of $H_{24}S_7X$, where X is the dopant

the QUANTUM ESPRESSO (QE) package, with Vanderbilt ultrasoft pseudopotentials [33]. We have adopted $\boldsymbol{k}$ mesh of $16 \times 16 \times 16$ and $\boldsymbol{q}$ mesh of $4 \times 4 \times 4$ and tested the convergence with $\boldsymbol{k}$ mesh of $20 \times 20 \times 20$ and $\boldsymbol{q}$ mesh of $5 \times 5 \times 5$ for $H_{24}S_7X$. For $H_{48}S_{15}X$, $\boldsymbol{k}$ mesh was used as $12 \times 12 \times 12$ and $\boldsymbol{q}$ mesh was used as $3 \times 3 \times 3$. The smearing method was Methfessel-Paxton first-order spreading [34] of 0.03 Ry. The cutoff energy for basis of plane waves was employed to be 100 Ry. Then, the transition temperatures were estimated by the McMillan-Allen-Dynes (MAD) formula [35],

$$T_c = f_1 f_2 \frac{\omega_{\ln}}{1.20} \exp\left[-\frac{1.04(1+\lambda)}{\lambda - \mu^*(1+0.62\lambda)}\right], \quad (1)$$

where

$$f_1 = \left\{1 + \left[\frac{\lambda}{2.46(1+3.8\mu^*)}\right]^{3/2}\right\}^{1/3},$$

$$f_2 = 1 + \frac{\lambda^2(\omega_2/\omega_{\ln} - 1)}{\lambda^2 + [1.82(1+6.3\mu^*)(\omega_2/\omega_{\ln})]^2} \quad (2)$$

are the correction factors. μ^*, λ, and $\omega_{\ln}$ indicate the screened Coulomb parameter, electron-phonon coupling constant, and the logarithm average over phonon frequency, respectively.

We have also computed the results by Migdal-Eliashberg (ME) theory [36–39],

$$Z(i\omega_j) = 1 + \frac{\pi T}{\omega_j} \sum_{j'} \frac{\omega_{j'}}{\sqrt{\omega_{j'}^2 + \Delta^2(i\omega_{j'})}} \lambda(i\omega_j - i\omega_{j'}), \quad (3)$$

$$Z(i\omega_j)\Delta(i\omega_j) = \pi T \sum_{j'} \frac{\Delta(i\omega_{j'})}{\sqrt{\omega_{j'}^2 + \Delta^2(i\omega_{j'})}} \times [\lambda(i\omega_j - i\omega_{j'}) - \mu^*], \quad (4)$$

$$\lambda(i\omega_j - i\omega_{j'}) = \int d\omega \frac{2\omega\alpha^2 F(\omega)}{\omega^2 + (\omega_j - \omega_{j'})^2} \quad (5)$$

to compare with that of the MAD equation, which is realized by the ELK code [40]. The T_c could be obtained once the superconducting gap $\Delta(i\omega_j)$ becomes zero in numerically solving ME equation.

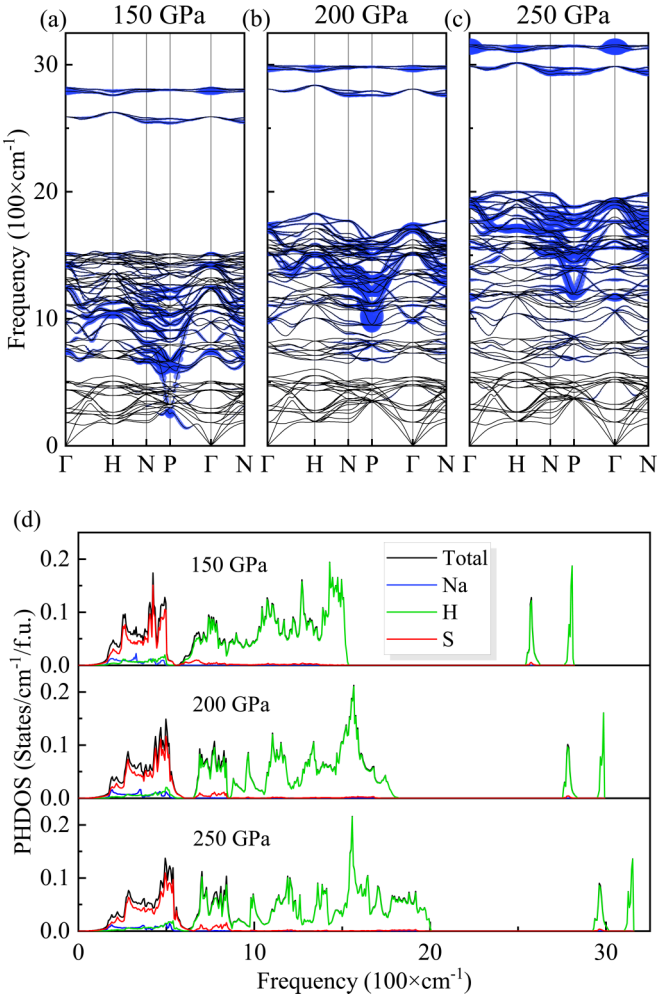

FIG. 2. Phonon dispersion and phonon linewidth for $H_{24}S_7Na$ at pressure (a) 150 GPa, (b) 200 GPa, and (c) 250 GPa; the magnitude of the phonon linewidth is indicated by the radii of blue circles. (d) Phonon density of states for $H_{24}S_7Na$ at 150–250 GPa.

III. RESULTS AND DISCUSSION

We began our simulations on investigating the validity of the supercell approach by computing the electronic properties and phonon properties of a primitive cell and a supercell of 32 atoms ($H_{24}S_8$) for H_3S at 200 GPa, as shown in Fig. S1 [41]. As shown in Fig. S2 [41], the superconductivity using the supercell is well consistent with that simulated from primitive cell of H_3S, which is also in agreement with previous results [2,3]. The relevant information is listed in Table S1 of the Supplemental Material [41].

Furthermore, we have systematically investigated the doping of H_3S by the elements from H to Cl without He and Ne in the Periodic Table using supercells of 32 and 64 atoms. The structures of $H_{24}S_7X$ and $H_{48}S_{15}X$ are provided in Fig. S3 [41]. The results indicate the doping could destabilize the structure for several compounds. For the $H_{24}S_7X$ compounds, for example, imaginary frequency was found for the Γ point with $X = H$, indicating dynamical instability. The dynamical stability of $H_{24}S_7X$ compounds within the range

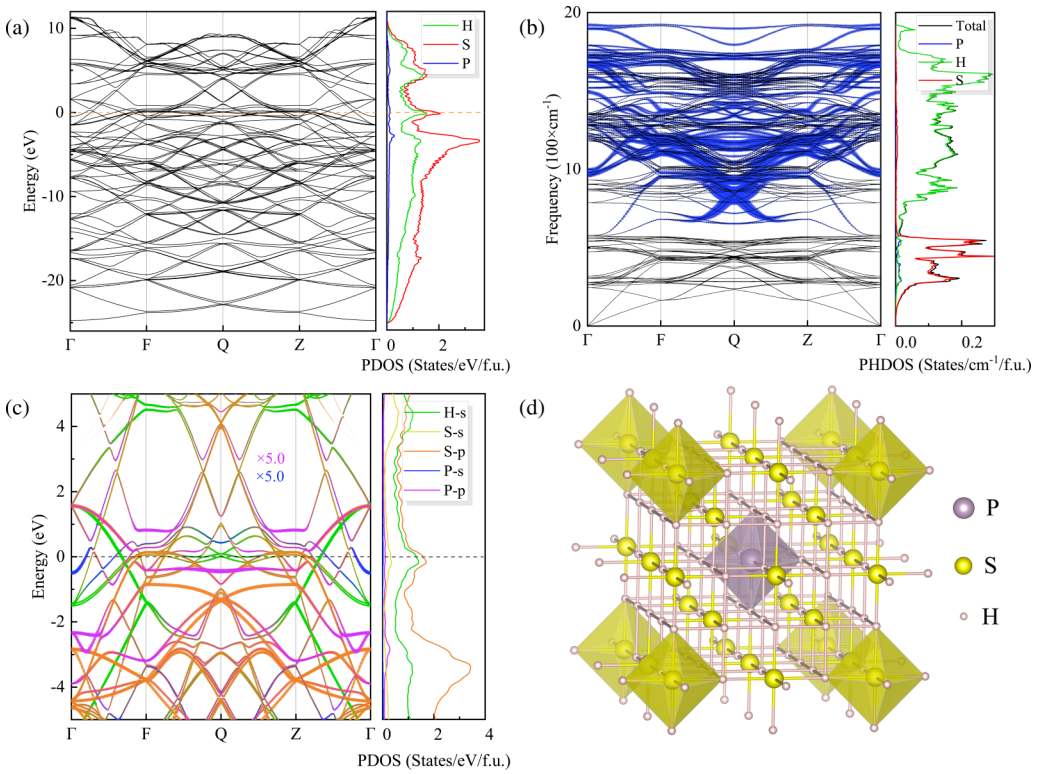

FIG. 3. (a) Electronic band structure (left panel) and projected density of states (right panel) of $H_{48}S_{15}P$ at 200 GPa. (b) Phonon dispersion with phonon linewidth (left panel) and phonon density of states (right panel) of $H_{48}S_{15}P$ at 200 GPa. The radii of the blue circles indicate the magnitude of the phonon linewidth. (c) Atom projected and orbital projected band structures (left panel) and density of states (right panel) of $H_{48}S_{15}P$ at 200 GPa near the Fermi surface. The width of the lines indicates the weights of the corresponding orbitals. Due to the low proportion of P atoms, their weights are displayed fivefold. (d) Crystal structure of $H_{48}S_{15}P$ at 200 GPa. The structures of $[PH_6]$ and $[SH_6]$ units are represented by the purple and yellow octahedra units respectively.

150–250 GPa is summarized in Fig. 1. Moreover, we found that 12.5% doping of Na into H_3S has a lower dynamical stable pressure (140 GPa) compared to 180 GPa of the parent H_3S [2]. The absence of imaginary phonon frequency in the simulated phonon dispersion implies the dynamical stability of $H_{24}S_7Na$, as shown in Fig. 2. It is clearly seen that the strongest electron-phonon interaction mainly emerges around the P point, which may lead to a large λ of 2.31. As a result, T_c of $H_{24}S_7Na$ can reach 191 K at 150 GPa by using ME equation with $\mu^* = 0.10$.

As shown in previous studies, the low-proportion P doped H_3S has the high superconductivity due to the enhanced density of states at the Fermi level of parent H_3S [42,43], even though superconductivity decreased by more than 12.5% P doping [44]. We have also performed the simulations for elucidating the physical mechanism of this compound by using a supercell of 64 atoms ($H_{48}S_{15}P$). As is shown in Figs. 3(a) and S4, there are several flat bands along the $\boldsymbol{k}$ path $F \rightarrow Q \rightarrow Z$ at the Fermi surface, with the derivative $\partial E_n/\partial k$ almost zero. This indicates that the doping of P alters the two Van Hove singularities [42,45] and can result in a peak of density of states right at the Fermi surface. Moreover, we found that the symmetry is preserved well after doping due to the existence of the near degeneracies in electronic band structures as shown in Fig. 3(a), which can also be a critical factor to induce Van Hove singularities [23]. The high electronic density of states at the Fermi level could contribute to the large magnitude of phonon linewidth, as shown in Fig. 3(b) and contrasted with Fig. S5 [41]. We have also found the hybridization of s orbitals of H with p orbitals of S and P near the Fermi surface [Fig. 3(c)]. The negligible curvature of the flat bands indicates well localization of corresponding s and p electrons, revealing the strong P-H and S-H chemical bondings. Figure 3(d) shows the existence of $[PH_6]$ and $[SH_6]$ units, where the distances between P-H and S-H are compressed to 1.470 and 1.474 Å, compared with 1.493 Å in H_3S and 1.494–1.511 Å for other S-H bonds in $H_{48}S_{15}P$. Finally, we found that the 6.25% P doping could enhance the T_c of H_3S around 20–30 K at 200 and 250 GPa.

To explore the superconductivity of the C-doped H_3S, we have computed the electron-phonon coupling strength of $H_{32}S_7C$, $H_{36}S_{11}C$, and $H_{48}S_{15}C$. For larger supercells corresponding to lower-proportion C-doped H_3S, the simulations could not be afforded due to computational demanding of these simulations as well as the limitation of our computational power. Therefore, we attempt to estimate the superconductivity of low-proportion C-doped H_3S without performing actual electron-phonon coupling simulations for a large supercell. Given that similar structures of the low-proportion C-doped H_3S share a similar magnitude of average mass and electron-phonon interaction at the same pressure, we could thus estimate λ of the MgB_2 type superconductors

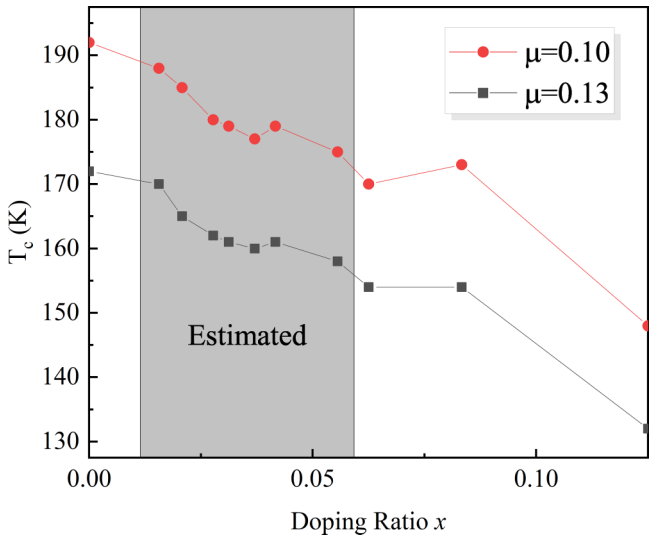

FIG. 4. Calculated x dependence of T_c for $H_3S_{1-x}C_x$ at 260 GPa. The points in the gray region are estimated by Eqs. (6) and (7).

by the Hopfield expression [46,47]

$$\lambda = \frac{N(0)I^2}{M\omega^2}. \tag{6}$$

Then, the T_c can be estimated by [47]

$$T_c = \omega \exp\left(-\frac{1}{\frac{\lambda}{1+\lambda} - \mu^*}\right). \tag{7}$$

Further details of our estimation approach is also provided in the Supplemental Material [41]. As is shown in Table S2, values of T_c computed from our approach vary only about 5% at maximum compared with that directly computed by QE, indicating the validity of our computational scheme. We thus investigated the superconductivity of the doping system of H_3S up to 256 atoms as shown in Table S3 and Fig. 4. The T_c of $H_3S_{1-x}C_x$ with $x = 0.1250$–0.0156 could reach 148–192 K with $\mu^* = 0.10$ at 260 GPa. This suggests that the estimated superconductivity of C-doped H_3S is much lower than room temperature as predicted in previous studies [22,23]. The reason for this discrepancy is possibly because different approaches were employed. As for other predicted compounds, the superconductivity-related information is included in Table I.

In addition, we have investigated the thermodynamic stability of all the predicted compounds. Given that H_3S is a highly likely decomposition compound, we considered the formation enthalpy as below:

$$\Delta H = \frac{H(H_3S_{1-x}X_x) + xH(S) - H(H_3S) - xH(X)}{4+x}. \tag{8}$$

As listed in Table S4 [41], the results indicate the $H_3S_{0.875}Na_{0.125}$ and $H_3S_{0.875}F_{0.125}$ have negative formation enthalpy. The formation enthalpy for P doped H_3S and $H_3S_{1-x}C_x$ with $x < 0.0833$ are below 50 meV/atom, indicating they are metastable phases, which are likely to be measured along a proper reaction path [43,48].

IV. CONCLUSION

In summary, we have computed the superconductivity of light-elements doped H_3S using a supercell approach within the framework of first-principle electronic structure. Our simulations indicate that the doping of Na can lower the dynamically stable pressure of H_3S while the doping of P can increase the density of states at the Fermi level as well as the

TABLE I. The parameters of the superconductivity for the doped H_3S at a pressure range of 150-250 GPa, where the typical screened Coulomb parameter μ^* of 0.1-0.13 is employed.

Dopant	Doping ratio	Pressure (GPa)	λ	$\omega_{\ln}$ (K)	$N(0)$ (states/Ry/atom)	T_c by MAD equation (K)	T_c by ME equation (K)
B	0.1250	200	1.56	1281	0.721	154–171	176–191
B	0.1250	250	1.21	1447	0.692	126–143	140–156
C	0.1250	250	1.40	1259	0.709	134–150	153–169
F	0.1250	250	1.04	1428	0.605	97–113	105–120
Na	0.1250	150	2.31	846	0.656	154–169	178–191
Na	0.1250	200	1.56	1094	0.660	133–148	149–167
Na	0.1250	250	1.42	1152	0.667	125–140	138–152
Si	0.1250	200	1.99	1155	0.838	182–199	210–225
Si	0.1250	250	1.59	1294	0.849	161–179	188–205
P	0.1250	200	2.02	1238	0.841	197–215	222–238
P	0.1250	250	1.53	1520	0.922	180–199	207–224
P	0.0625	200	2.29	1193	0.933	212–231	246–262
P	0.0625	250	1.66	1512	0.955	196–216	227–244
Cl	0.1250	200	1.31	1424	0.706	137–154	153–168
Cl	0.1250	250	1.08	1591	0.700	115–133	129–145
S		200	1.85	1358	0.868	195–214	222–238
S		250	1.46	1571	0.875	175–195	197–219

superconductivity of H_3S. Remarkably, we found that the existence of octahedra [PH_6] and [SH_6] units with squeezed P-H and S-H bonds in $H_{48}S_{15}P$ which are likely to be related to the high density of states at the Fermi level, with the higher T_c of 20–30 K compared with H_3S. Furthermore, we have proposed an estimation approach to reasonably estimate the superconductivity of the low proportion C-doping H_3S without performing electron-phonon calculations for a quite large supercell. Our current work may inspire future work toward searching for high-temperature superconductivity in light-elements doping systems.

ACKNOWLEDGMENTS

This work was supported by the Major Program of the National Natural Science Foundation of China (Grant No. 52090024), National Natural Science Foundation of China (Grants No. 12074138, No. 11874175, and No. 11874176), Fundamental Research Funds for the Central Universities (Jilin University, JLU), Program for JLU Science and Technology Innovative Research Team (JLUSTIRT), and The Strategic Priority Research Program of Chinese Academy of Sciences (Grant No. XDB33000000). This work used computing facilities at the High-Performance Computing Centre of Jilin University.

[1] Y. Li, J. Hao, H. Liu, Y. Li, and Y. Ma,The metallization and superconductivity of dense hydrogen sulfide, J. Chem. Phys. **140**, 174712 (2014).

[2] D. Duan, Y. Liu, F. Tian, D. Li, X. Huang, Z. Zhao, H. Yu, B. Liu, W. Tian, and T. Cui, Pressure-induced metallization of dense $(H_2S)_2H_2$ with high-Tc superconductivity, Sci. Rep. **4**, 6968 (2014).

[3] A. P. Drozdov, M. I. Eremets, I. A. Troyan, V. Ksenofontov, and S. I. Shylin, Conventional superconductivity at 203 kelvin at high pressures in the sulfur hydride system, Nature (London) **525**, 73 (2015).

[4] Y. Li, J. Hao, H. Liu, J. S. Tse, Y. Wang, and Y. Ma, Pressure-stabilized superconductive yttrium hydrides, Sci. Rep. **5**, 9948 (2015).

[5] H. Liu, I. I. Naumov, R. Hoffmann, N. W. Ashcroft, and R. J. Hemley, Potential high-Tc superconducting lanthanum and yttrium hydrides at high pressure, Proc. Natl. Acad. Sci. USA **114**, 6990 (2017).

[6] F. Peng, Y. Sun, C. J. Pickard, R. J. Needs, Q. Wu, and Y. Ma, Hydrogen Clathrate Structures in Rare Earth Hydrides at High Pressures: Possible Route to Room-Temperature Superconductivity, Phys. Rev. Lett. **119**, 107001 (2017).

[7] M. Somayazulu, M. Ahart, A. K. Mishra, Z. M. Geballe, M. Baldini, Y. Meng, V. V. Struzhkin, and R. J. Hemley, Evidence for Superconductivity above 260 K in Lanthanum Superhydride at Megabar Pressures, Phys. Rev. Lett. **122**, 027001 (2019).

[8] A. P. Drozdov, P. P. Kong, V. S. Minkov, S. P. Besedin, M. A. Kuzovnikov, S. Mozaffari, L. Balicas, F. F. Balakirev, D. E. Graf, V. B. Prakapenka, E. Greenberg, D. A. Knyazev, M. Tkacz, and M. I. Eremets, Superconductivity at 250 K in lanthanum hydride under high pressures, Nature (London) **569**, 528 (2019).

[9] D. V. Semenok, A. G. Kvashnin, A. G. Ivanova, V. Svitlyk, V. Y. Fominski, A. V. Sadakov, O. A. Sobolevskiy, V. M. Pudalov, I. A. Troyan, and A. R. Oganov, Superconductivity at 161 K in thorium hydride ThH_{10}: Synthesis and properties, Mater. Today **33**, 36 (2020).

[10] P. P. Kong, V. S. Minkov, M. A. Kuzovnikov, S. P. Besedin, A. P. Drozdov, S. Mozaffari, L. Balicas, F. F. Balakirev, V. B. Prakapenka, E. Greenberg, D. A. Knyazev, and M. I. Eremets, Superconductivity up to 243 K in yttrium hydrides under high pressure, Nat. Commun. **12**, 5075 (2021).

[11] Y. Sun, J. Lv, Y. Xie, H. Liu, and Y. Ma, Route to a Superconducting Phase above Room Temperature in Electron-Doped Hydride Compounds under High Pressure, Phys. Rev. Lett. **123**, 097001 (2019).

[12] E. Snider, N. Dasenbrock-Gammon, R. McBride, M. Debessai, H. Vindana, K. Vencatasamy, K. V. Lawler, A. Salamat, and R. P. Dias, Room-temperature superconductivity in a carbonaceous sulfur hydride, Nature (London) **586**, 373 (2020).

[13] J. A. Flores-Livas, L. Boeri, A. Sanna, G. Profeta, R. Arita, and M. Eremets, A perspective on conventional high-temperature superconductors at high pressure: Methods and materials, Phys. Rep. **856**, 1 (2020).

[14] J. Lv, Y. Sun, H. Liu, and Y. Ma, Theory-orientated discovery of high-temperature superconductors in superhydrides stabilized under high pressure, Matter Radiat. Extremes **5**, 068101 (2020).

[15] E. Zurek and T. Bi, High-temperature superconductivity in alkaline and rare earth polyhydrides at high pressure: A theoretical perspective, J. Chem. Phys. **150**, 050901 (2019).

[16] H. Wang, J. S. Tse, K. Tanaka, T. Iitaka, and Y. Ma, Superconductive sodalite-like clathrate calcium hydride at high pressures, Proc. Natl. Acad. Sci. USA **109**, 6463 (2012).

[17] L. Ma, K. Wang, Y. Xie, X. Yang, Y. Wang, M. Zhou, H. Liu, G. Liu, H. Wang, and Y. Ma, Experimental observation of superconductivity at 215 K in calcium superhydride under high pressures, arXiv:2103.16282.

[18] Z. W. Li, X. He, C. L. Zhang, S. J. Zhang, S. M. Feng, X. C. Wang, R. C. Yu, and C. Q. Jin, Superconductivity above 200 K observed in superhydrides of calcium, arXiv:2103.16917.

[19] Y. Sun, Y. Tian, B. Jiang, X. Li, H. Li, T. Iitaka, X. Zhong, and Y. Xie, Computational discovery of a dynamically stable cubic SH_3-like high-temperature superconductor at 100 GPa via CH_4 intercalation, Phys. Rev. B **101**, 174102 (2020).

[20] W. Cui, T. Bi, J. Shi, Y. Li, H. Liu, E. Zurek, and R. J. Hemley, Route to high-T_c superconductivity via CH_4-intercalated H_3S hydride perovskites, Phys. Rev. B **101**, 134504 (2020).

[21] S. X. Hu, R. Paul, V. V. Karasiev, and R. P. Dias, Carbon-doped sulfur hydrides as room-temperature superconductors at 270 GPa, arXiv:2012.10259.

[22] M. Dogan and M. L. Cohen, Anomalous behavior in high-pressure carbonaceous sulfur hydride, Physica C **583**, 1353851 (2021).

[23] T. Wang, M. Hirayama, T. Nomoto, T. Koretsune, R. Arita, and J. A. Flores-Livas, Absence of conventional room-temperature superconductivity at high pressure in carbon-doped H_3S, Phys. Rev. B **104**, 064510 (2021).

[24] E. Bykova, M. Bykov, S. Chariton, V. B. Prakapenka, K. Glazyrin, A. Aslandukov, A. Aslandukova, G. Criniti, A. Kurnosov, and A. F. Goncharov, Structure and composition of C-S-H compounds up to 143 GPa, Phys. Rev. B **103**, L140105 (2021).

[25] M. Du, Z. Zhang, T. Cui, and D. Duan, Superconductivity of CH_4-intercalated H_3S under high pressure, arXiv:2107.10485.

[26] Y. Ge, F. Zhang, R. P. Dias, R. J. Hemley, and Y. Yao, Hole-doped room-temperature superconductivity in $H_3S_{1-x}Z_x$ (Z=C, Si), Mater. Today Phys. **15**, 100330 (2020).

[27] L. Nordheim, Zur Elektronentheorie der Metalle. I, Ann. Phys. **401**, 607 (1931).

[28] G. Kresse and J. Furthmüller, Efficient iterative schemes for ab initio total-energy calculations using a plane-wave basis set, Phys. Rev. B **54**, 11169 (1996).

[29] J. P. Perdew, K. Burke, and M. Ernzerhof, Generalized Gradient Approximation Made Simple, Phys. Rev. Lett. **77**, 3865 (1996).

[30] P. E. Blöchl, Projector augmented-wave method, Phys. Rev. B **50**, 17953 (1994).

[31] H. J. Monkhorst and J. D. Pack, Special points for Brillouin-zone integrations, Phys. Rev. B **13**, 5188 (1976).

[32] V. Wang, N. Xu, J.-C. Liu, G. Tang, and W.-T. Geng, VASPKIT: A user-friendly interface facilitating highthroughput computing and analysis using VASP code, Comput. Phys. Commun. **267**, 108033 (2021).

[33] D. Vanderbilt, Soft self-consistent pseudopotentials in a generalized eigenvalue formalism, Phys. Rev. B **41**, 7892 (1990).

[34] M. Methfessel and A. T. Paxton, High-precision sampling for Brillouin-zone integration in metals, Phys. Rev. B **40**, 3616 (1989).

[35] P. B. Allen and R. C. Dynes, Transition temperature of strong-coupled superconductors reanalyzed, Phys. Rev. B **12**, 905 (1975).

[36] A. B. Migdal, Interaction between electrons and lattice vibrations in a normal metal, Sov. Phys. JETP **34**, 996 (1958).

[37] G. M. Eliashberg, Interactions between electrons and lattice vibrations in a superconductor, Sov. Phys. JETP **11**, 696 (1960).

[38] D. J. Scalapino, J. R. Schrieffer, and J. W. Wilkins, Strong-coupling superconductivity. I, Phys. Rev. **148**, 263 (1966).

[39] A. Sanna, S. Pittalis, J. K. Dewhurst, M. Monni, S. Sharma, G. Ummarino, S. Massidda, and E. K. U. Gross, Phononic self-energy effects and superconductivity in CaC_6, Phys. Rev. B **85**, 184514 (2012).

[40] The Elk Code, http://elk.sourceforge.net/.

[41] See Supplemental Material at http://link.aps.org/supplemental/10.1103/PhysRevResearch.3.043102 for analysis of Allen-Dynes-McMillan equation, estimation method and results for C doped H_3S, crystal structures, electronic properties, phonon properties, and formation enthalpy.

[42] Y. Ge, F. Zhang, and Y. Yao, First-principles demonstration of superconductivity at 280 K in hydrogen sulfide with low phosphorus substitution, Phys. Rev. B **93**, 224513 (2016).

[43] A. Nakanishi, T. Ishikawa, and K. Shimizu, First-principles study on superconductivity of P- and Cl-doped H_3S, J. Phys. Soc. Jpn. **87**, 124711 (2018).

[44] A. P. Durajski and R. Szczeniak, Gradual reduction of the superconducting transition temperature of H_3S by partial replacing sulfur with phosphorus, Phys. C (Amsterdam, Neth.) **554**, 38 (2018).

[45] Y. Quan and W. E. Pickett, Van Hove singularities and spectral smearing in high-temperature superconducting H_3S, Phys. Rev. B **93**, 104526 (2016).

[46] J. J. Hopfield, Angular momentum and transition-metal superconductivity, Phys. Rev. **186**, 443 (1969).

[47] L. Boeri, J. Kortus, and O. K. Andersen, Three-Dimensional MgB_2-Type Superconductivity in Hole-Doped Diamond, Phys. Rev. Lett. **93**, 237002 (2004).

[48] P. Tsuppayakorn-aek, P. Phansuke, P. Kaewtubtim, R. Ahuja, and T. Bovornratanaraks, Enthalpy stabilization of superconductivity in an alloying S-P-H system: First-principles cluster expansion study under high pressure, Comput. Mater. Sci. **190**, 110282 (2021).